Available online at www.sciencedirect.com
ScienceDirect
Journal of Molecular Catalysis A: Chemical 272 (2007) 45–52
JOURNAL OF MOLECULAR CATALYSIS A: CHEMICAL
www.elsevier.com/locate/molcata

Review

Synthesis, characterization and catalytic activity of $Au/Ce_{0.8}Zr_{0.2}O_2$ catalysts for CO oxidation

Shu-Ping Wang, Tong-Ying Zhang, Xiao-Ying Wang, Shou-Min Zhang, Shu-Rong Wang, Wei-Ping Huang, Shi-Hua Wu *

Department of Chemistry, Nankai University, Tianjin 300071, China

Received 31 January 2007; received in revised form 8 March 2007; accepted 8 March 2007
Available online 15 March 2007

Abstract

Nanostructure $Ce_{0.8}Zr_{0.2}O_2$ powders used as the support were synthesized by a hydrothermal route and the $Au/Ce_{0.8}Zr_{0.2}O_2$ catalysts were prepared via deposition-precipitation method. The samples were characterized by X-ray diffraction pattern (XRD), Fourier transform Raman spectra (FT-Raman), high-resolution transmission electron microscope (HRTEM), X-ray photoelectron spectra (XPS) and temperature-programmed reduction (TPR) techniques. The influence of the pH values, Au loadings, calcination temperature and calcination time on the catalytic activity of the $Au/Ce_{0.8}Zr_{0.2}O_2$ catalysts was investigated. The suitable pH value to prepare the catalysts was 7.0 and the suitable calcination conditions were 300 °C and 3 h. The Au(2 wt.%)/$Ce_{0.8}Zr_{0.2}O_2$ catalyst showed the best catalytic performance among all the prepared samples. TPR analysis indicated that the addition of gold can improve the reducibility of the catalyst obviously. XPS analysis revealed that both Ce^{4+} and Ce^{3+} were present on the surface of the catalyst. According to TPR and XPS analyses, the gold particles (Au^0 and Au^{3+}) existed in the catalyst, which played an important role in the catalytic activity. XRD and XPS results showed that the high dispersion degree of gold particles on the support was responsible for the superior catalytic property.

Keywords: $Au/Ce_{0.8}Zr_{0.2}O_2$ catalysts; Gold particle; CO oxidation; Catalytic activity

Contents

1. Introduction

Cerium dioxide containing materials have been the subject of numerous investigations in recent years. Ceria is an interesting oxide in the three-way catalysts (TWCs) used for eliminating

* Corresponding author. Tel.: +86 22 23505896; fax: +86 22 23502458.
E-mail address: wushh@nankai.edu.cn (S.-H. Wu).

1381-1169/$ – see front matter © 2007 Elsevier B.V. All rights reserved.
doi:10.1016/j.molcata.2007.03.027

toxic gases in automobile exhaust. The success of ceria is mainly due to the enhancement of the metal dispersion, the application in the water–gas shift reaction and the oxygen storage capacity provided by the redox couple Ce^{4+}/Ce^{3+} [1–3]. Despite of its widespread applications, the use of pure cerium dioxide is highly discouraged because of its poor thermal stability [4,5]. To solve this problem, one way is to associate ceria to other elements for obtaining solid solutions with improved thermal properties. Many studies have focused on the zirconia–ceria solid solutions [5–8]. Because of their high OSC, redox property, thermal resistance and better catalytic activity at lower temperatures, the zirconia–ceria has been applied widely as a component of TWCs for the treatment of automotive exhaust gases.

Precious metals are well-known oxidation catalysts with high activity and widely used for CO oxidation reaction. Pt, Pd, Rh, Au loaded catalysts have been reported by many investigations [9–12]. However, few literatures have reported the study of Au supported on ceria-zirconia as catalysts for low-temperature CO oxidation.

The present paper reported the study of the catalysts $Au/Ce_{0.8}Zr_{0.2}O_2$ on the catalytic performance for CO oxidation. The support $Ce_{0.8}Zr_{0.2}O_2$ was prepared via a hydrothermal route and the $Au/Ce_{0.8}Zr_{0.2}O_2$ catalysts were synthesized by a deposition-precipitation method. The samples were characterized by XRD, FT-Raman, HRTEM, XPS and TPR techniques. The catalytic activities of the catalysts were evaluated by using a microreactor-GC system. The influence of the pH values, Au contents, calcination temperature and calcination time on the catalytic property for low-temperature CO oxidation is discussed in this paper.

2. Experimental

2.1. Preparation of support and catalyst

The support $Ce_{0.8}Zr_{0.2}O_2$ was prepared via a hydrothermal route by using $Ce(NO_3)_3{\cdot}6H_2O$, $Zr(NO_3)_4{\cdot}5H_2O$ as precursors. 2.78 g $Ce(NO_3)_3{\cdot}6H_2O$ and 0.69 g $Zr(NO_3)_4{\cdot}5H_2O$ were dissolved into 80 ml distilled water in a Teflon bottle with an inner volume of 100 ml. A transparent solution was obtained under vigorous stirring. Then 0.96 g urea ($CO(NH_2)_2$) was slowly added into the above solution. The addition was carried out under agitation in order to keep the local concentration homogeneous. While stirring for about 1 h, the Teflon bottle was put in a stainless-steel autoclave and sealed tightly. Then it was put in an oven and the hydrothermal treatment at temperature of 160 °C for 24 h was performed. After the hydrothermal treatment, white precipitates were formed. The precipitates were separated by centrifuging and washed with deionized water several times. They were dried at 80 °C overnight in the oven and then calcined at 500 °C in the muffle furnace for 4 h; yellow powder was obtained.

The $Au/Ce_{0.8}Zr_{0.2}O_2$ catalysts were prepared via a deposition-precipitation method. 0.3 g $Ce_{0.8}Zr_{0.2}O_2$ support was slurred in 10 ml distilled water. 0.39 g $HAuCl_4{\cdot}4H_2O$ was dissolved into 38 ml distilled water to form $HAuCl_4$ solution (0.21 mol/ml). Then calculated volume $HAuCl_4$ solution was slowly added into the support by separating funnel under vigorous stirring. At the same time, the pH was adjusted to 7.0 by the addition of $NH_3{\cdot}H_2O$ (0.1 M) and kept stirring for about 1 h. The above solution was centrifuged, and washed with deionized water until chloride ions cannot be detected using $AgNO_3$ solution. The production was dried at 70 °C overnight in the oven and then calcined at 300 °C in a muffle furnace for 3 h. For comparative study, a series of samples were also prepared at different pH value and calcined at different temperature and time.

2.2. Catalyst characterization

The high-resolution transmission electron microscope (HRTEM) was performed with a Philips T20ST transmission electron microscope operated at 200 kV. The X-ray diffraction patterns (XRD) were operated by using a DMAX-2500 diffractometer with Cu Kα radiation. The working voltage and current of the X-ray tube were 40 kV and 100 mA. The average crystalline size was calculated from the X-ray line broadening, according to Scherrer's equation. Fourier transform Raman spectra (FT-Raman) were recorded with a RTS 100/S FT-RAMAN spectrometer (BRUKER, Germany) with liquid N_2 detector, using the 1064 nm excitation line of Nd-YAG laser. The sample powders were pressed into small disc and then mounted on the analytic chamber. X-ray photoelectron spectra (XPS) were analyzed on a PHI-1600 spectrometer (U.S.A.) equipped with Mg Kα radiation for exciting photoelectrons. X-ray source was operated at an accelerating voltage of 15 kV and 250 W. The pressure in the ion-pumped analysis chamber was maintained at 1.1×10^{-7} during data acquisition. All binding energies (BE) were referenced to the adventitious C 1s line at 284.6 eV (1 eV = 1.602×10^{-19} J). Temperature-programmed reduction (TPR) experiments were performed on a TPDRO 1100 apparatus supplied by Thermo-Finnigan Company. Fifty milligrams of the sample was heated from room temperature to 1000 °C at a rate of 10 °C/min under the mixture of 5% H_2 in N_2 flowing (20 ml/min). The H_2 uptake amount during the reduction was measured by a gas chromatograph equipped with a thermal conductivity detector (TCD).

2.3. Catalytic activity test

The catalytic activity measurements of the prepared catalysts for CO oxidation were tested using a fixed bed flow microreactor (7 mm i.d.) under atmospheric pressure. 0.05 g catalyst powder was mixed with 2.00 g SiO_2 uniformly. The airflow rate was 33.3 ml/min, and the CO gas flow rate was 0.5 ml/min. The reactant and product composition were analyzed on-line by a GC-508A gas chromatograph equipped with a thermal conductivity detector.

3. Result and discussion

3.1. Characterization of catalysts

Figs. 1 and 2 depict the XRD patterns of the catalysts with different Au loadings and prepared at different pH values,

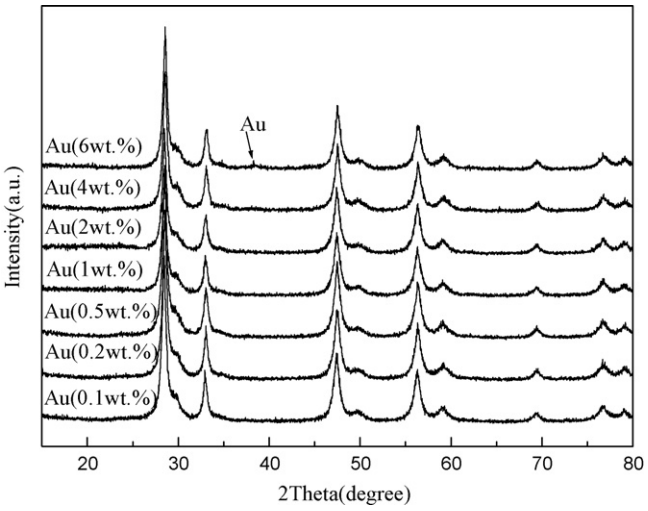

Fig. 1. XRD patterns of the Au/$Ce_{0.8}Zr_{0.2}O_2$ catalysts with different Au loadings.

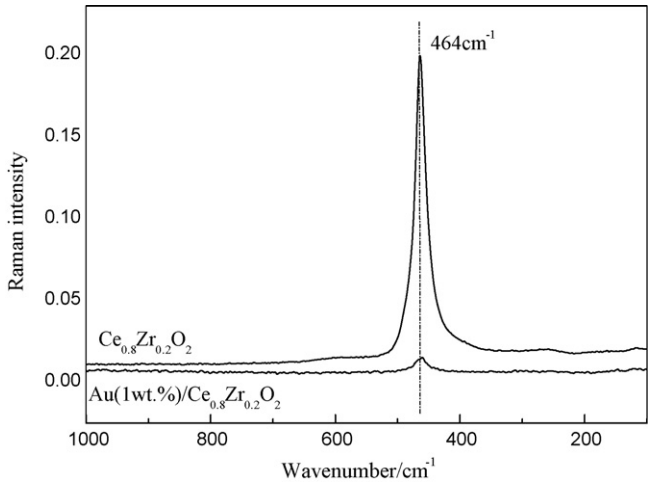

Fig. 3. The FT-Raman spectra of the support $Ce_{0.8}Zr_{0.2}O_2$ and the catalyst Au(1 wt.%)/$Ce_{0.8}Zr_{0.2}O_2$.

respectively. Diffractions attributed to the typical structure of CeO_2 (true cubic, fluorite structure) were clearly detectable for all the catalysts, which indicated that the zirconia dopant was contained within the lattice and not as a separate phase [5]. The same result can be confirmed by Raman spectroscopy (Fig. 3). From Fig. 1, no obvious peaks attributed to Au particles can be observed for the catalysts up to 4 wt.% gold suggesting a well-dispersed state of the gold particles on the support. When the Au loading increased to 6 wt.%, a small peak corresponding to Au(1 1 1) can be detected at $2\theta = 38.3^\circ$. We think that the agglomeration of gold particles on the surface of the support occur with the increase of gold loadings, which may have negative effect on the catalytic activities for CO oxidation. From Fig. 2, we can find that the catalysts with the pH > 6 could not produce reflections characteristic of the Au particles. But for the catalyst with pH 6, a weak peak can be observed at $2\theta = 38.3^\circ$, which was the (1 1 1) plane of gold particles. When the pH was 5, the peak attributed to the gold particles at $2\theta = 38.3^\circ$ was obvious. The results indicated that the pH values adjusted in the process of preparation were mainly responsible for the dispersion degree of gold particles. The average particle sizes of the support calculated from line broadening of (1 1 1) diffraction peak by using Scherrer equation were similar and about 15.1 nm, which indicated that the addition of gold should have no effect on the size and structure of the support. The same result was reported by Flytzani-Stephanopoulos and coworkers [13].

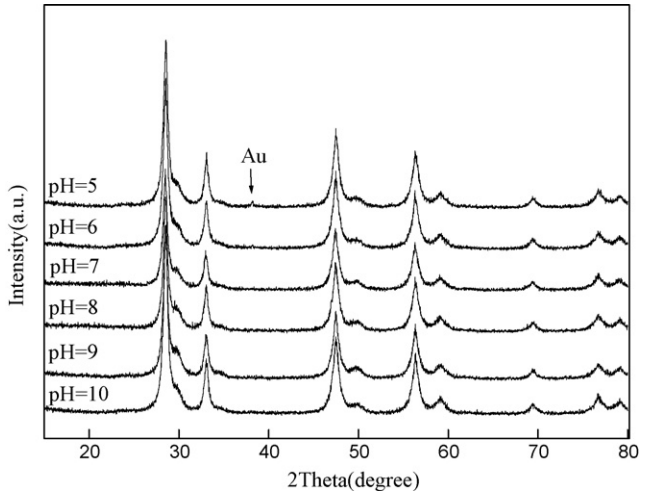

Fig. 2. XRD patterns of the Au/$Ce_{0.8}Zr_{0.2}O_2$ catalysts with different pH values.

The FT-Raman spectra of the support $Ce_{0.8}Zr_{0.2}O_2$ and the catalyst Au(1 wt.%)/$Ce_{0.8}Zr_{0.2}O_2$ (pH 7) are shown in Fig. 3. We can find that there was only one adsorption peak centered at about 464 cm^{-1} for the samples, which was typical of the F_{2g} Raman active mode of a fluorite structured material [14]. The result was in good agreement with the XRD analysis, which also indicated the presence of only the cubic fluorite structure type for the support of all the catalysts. Furthermore, the different intensity of the two samples can be observed. Because the atomic mass of Au is larger than that of Ce and Zr, we think the insertion of Au ions can decrease the vibration frequency of metal–anion band and thus decrease the intensity of the catalyst.

Fig. 4 shows the HRTEM micrographs of the support $Ce_{0.8}Zr_{0.2}O_2$ (a) and the catalyst Au(1 wt.%)/$Ce_{0.8}Zr_{0.2}O_2$ (pH 7) (b–d). Viewed at lower magnifications (Fig. 4a and b), the two samples appeared to be spherical particles, which indicated that the addition of Au had no influence on the morphology of the support. The average particle sizes estimated from the HRTEM were about 15 nm and agreed well with that calculated from the Scherrer equation. From Fig. 4c and d, the encircled darker particles could be discerned, but whether they were gold or smaller ceria particles was difficult to determine from the contrast. We think most of the gold particles could be much smaller and not detectable or they were less due to the lower Au loading. Furthermore, we can obtain the interplanar spacing (ca. 0.32 nm) from Fig. 4d, corresponding to the value of the (1 1 1) facet of cubic, fluorite structure of CeO_2. This can also be the identification for $Ce_{0.8}Zr_{0.2}O_2$ structure which was in agreement with the result of the XRD analysis.

XPS analysis showed in Fig. 5 reveals the presence of cerium, zirconium, gold and oxygen on the surface of the catalyst

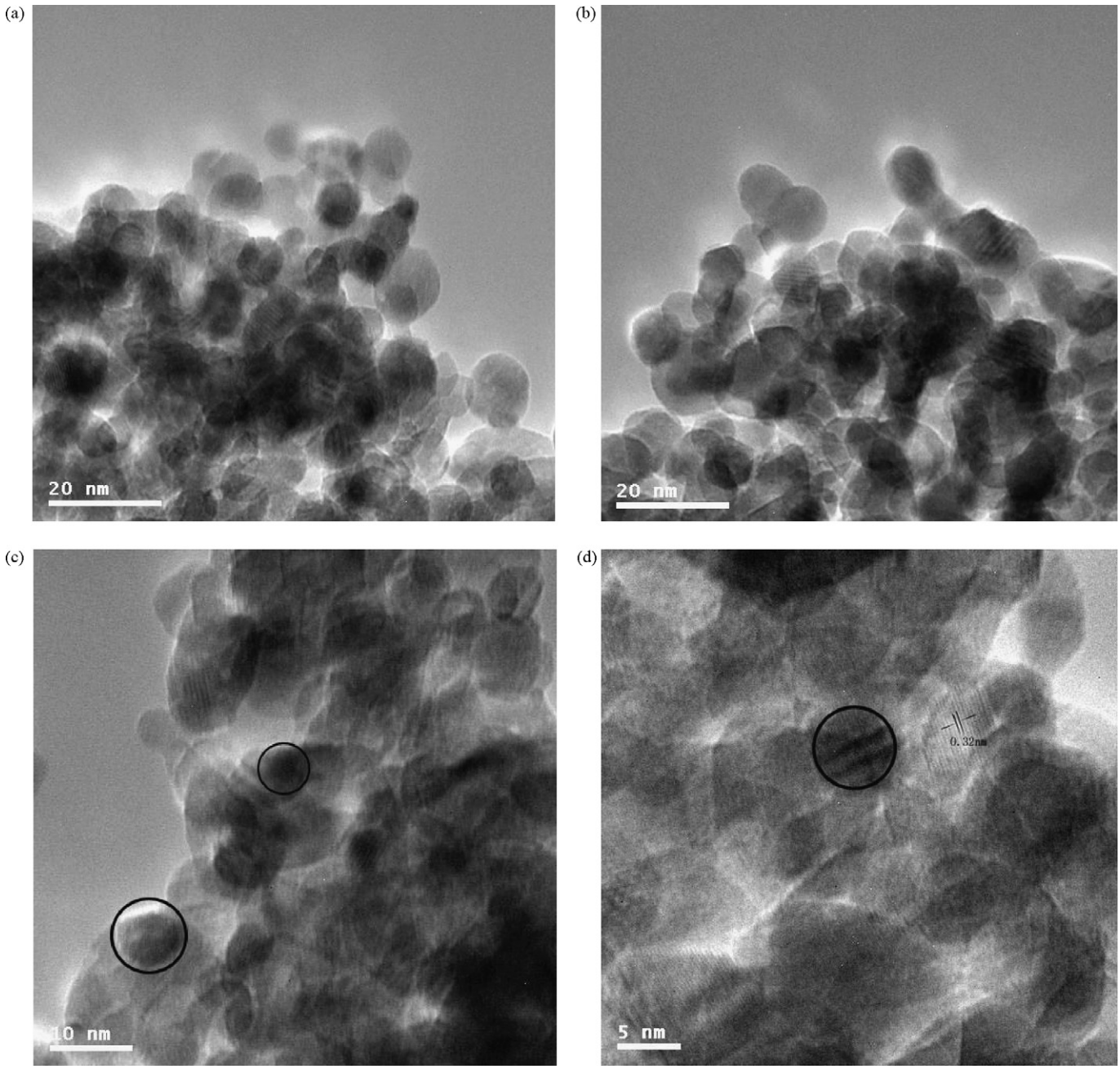

Fig. 4. HRTEM micrographs of the support $Ce_{0.8}Zr_{0.2}O_2$ (a) and the catalyst Au(1 wt.%)/$Ce_{0.8}Zr_{0.2}O_2$ (pH 7) (b–d).

Au(1 wt.%)/$Ce_{0.8}Zr_{0.2}O_2$ (pH 7) calcined at 300 °C for 3 h. The XP spectrum of cerium 3d (Fig. 5a) showed two principle binding energies of Ce $3d_{3/2}$ and Ce $3d_{5/2}$ at about 900.6 and 882 eV, respectively. The difference of the binding energies between the Ce $3d_{3/2}$ and Ce $3d_{5/2}$ photoemission feature was about 18.6 eV, which was in agreement with the reported value [15]. The peak at about 916 eV was the satellite arising from the Ce $3d_{3/2}$ ionization, while bands 885.2 and 898 eV were that of the Ce $3d_{5/2}$ ionization. The main peaks at about 916 and 898 eV represented the $3d^{10}4f^0$ initial electronic state corresponding to the Ce^{4+} ion, while a small peak at about 885.2 eV represented the $3d^{10}4f^1$ initial electronic state corresponding to the Ce^{3+} ion. The XP spectrum of Ce 3d exhibited peaks due to the presence of both Ce^{4+} and Ce^{3+}, thus implying that both Ce^{4+} and Ce^{3+} presented on the surface of the catalyst. Reddy and Khan [16] considered that the reduction of Ce^{4+} may occur under the procedure of XPS measurement. Delmon and coworkers [17] also considered that partial reduction could occur during the analysis if the exposure of the sample to exciting X-ray beam was long, and caused local heating of the sample. The XP spectrum of zirconium is showed in Fig. 5b, the double peaks at about 182.0 and 184.4 eV corresponded to the Zr $3d_{5/2}$ and Zr $3d_{3/2}$, respectively. The difference between the two peaks was in agreement with an expected value of about 2.4 eV [15]. The O 1s spectrum of the sample (Fig. 5c) showed two peaks, one main peak appearing at 529.5 eV represented the lattice oxygen associated

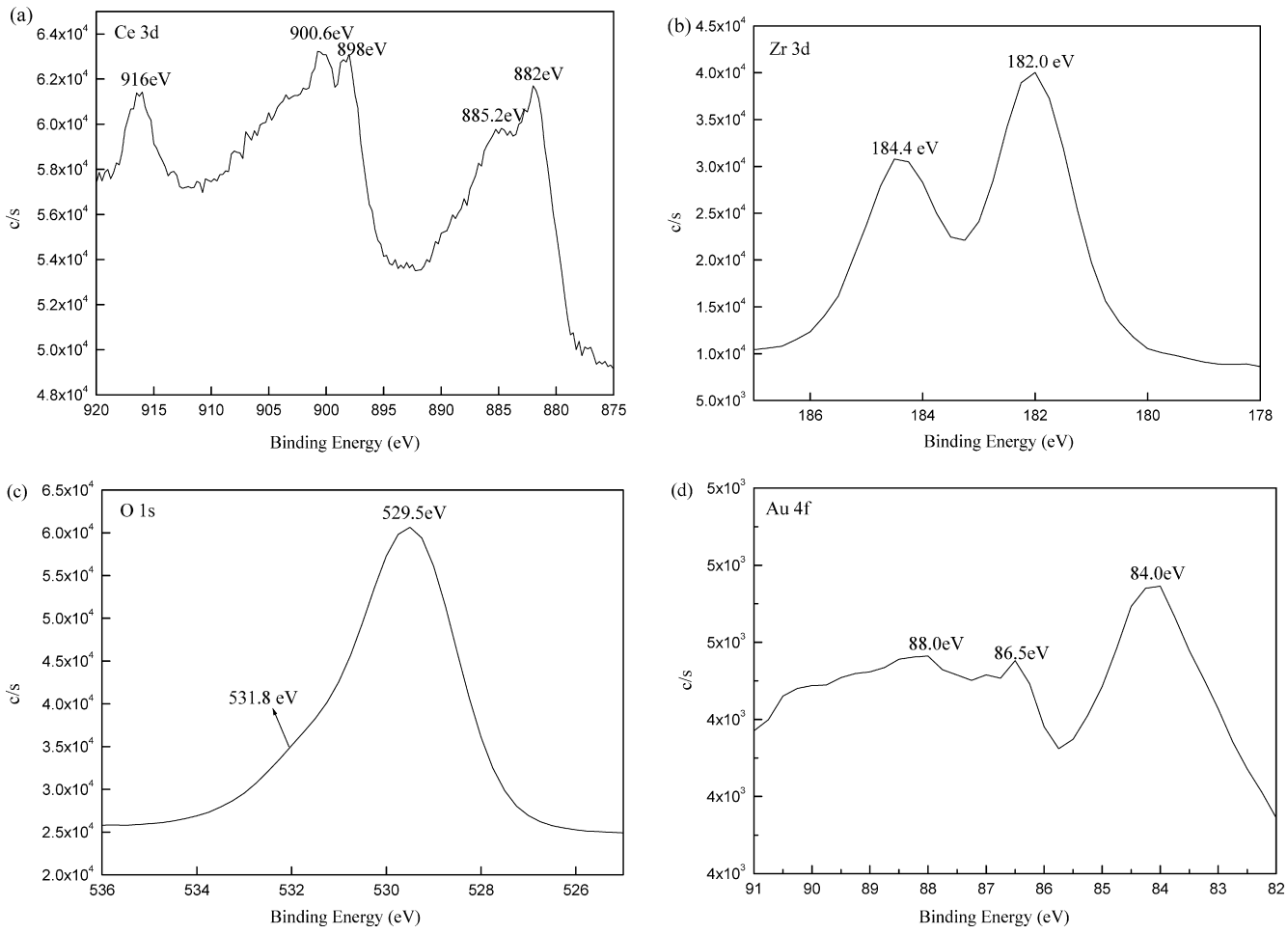

Fig. 5. XPS pattern of Au(1 wt.%)/$Ce_{0.8}Zr_{0.2}O_2$: (a) Ce 3d, (b) Zr 3d, (c) O 1s and (d) Au 4f.

with metal oxides and a shoulder peak at about 531.8 eV was attributed to the absorbed oxygen [5]. The Au 4f XP spectrum of the catalyst shown in Fig. 5d consisted of two Au $4f_{7/2}$ and one Au $4f_{5/2}$ peaks. The peaks at about 84.0 and 88.0 eV were corresponded to the Au $4f_{7/2}$ and Au $4f_{5/2}$, respectively, suggesting the Au^0 presented on the surface of the catalyst. While another Au $4f_{7/2}$ component at about 86.5 eV can be assigned to Au^{3+} species [18]. There was no indication of the presence of other Au species such as Au^{1+}. Bond and Thompson proposed that both Au^0 and Au^{3+} were required for high activity. They considered that Au^0 adsorbed CO, while Au^{3+} cemented the metallic particle on the support and activated surface hydroxyl groups, which can react with the adsorbed CO to form adsorbed carboxylate [19]. However, whether ionic or metallic gold is important for high activity has been disputed. We think that the highly dispersed gold particles (Au^0 and Au^{3+}) were responsible for the superior catalytic performance, which was consistent with the XRD analysis. The surface chemical composition of the catalyst was also investigated by XPS. The Au/(Ce + Zr) atomic ratio value was 0.0067, which was in good agreement with that expected value for the bulk composition of the sample with 1.0 wt.% Au content (Au/(Ce + Zr) = 0.0066).

The TPR profiles of the catalyst Au(1 wt.%)/$Ce_{0.8}Zr_{0.2}O_2$ (pH 7) and the support $Ce_{0.8}Zr_{0.2}O_2$ are shown in Fig. 6. Yao and Yao [20] have reported that the low-temperature reduction peak at 570 °C and the high temperature peak at 830 °C were typically interpreted as the reduction of surface-capping oxygen and bulk-phase lattice oxygen, respectively. Kang and Wan [21] reported that reduction peaks of Au at about 125 and 525 °C

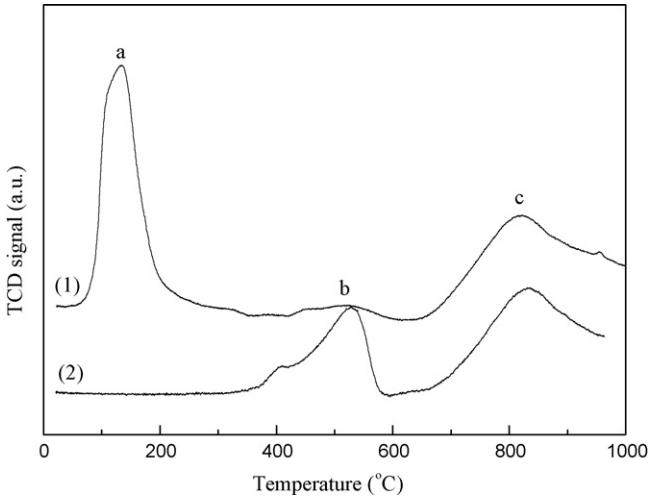

Fig. 6. TPR profiles of the catalysts: (1) Au(1 wt.%)/$Ce_{0.8}Zr_{0.2}O_2$; (2) $Ce_{0.8}Zr_{0.2}O_2$.

could be observed, which attributed to oxygen adsorbed on the surface of metallic gold and the reduction of Au^{3+}, respectively. In Fig. 6, it can be seen that for the support $Ce_{0.8}Zr_{0.2}O_2$ there were two obvious bands at about 530 °C (b) and 830 °C (c). While two main reduction peaks can be observed at 134 °C (a) and 822 °C (c) obviously for Au(1 wt.%)/$Ce_{0.8}Zr_{0.2}O_2$ and a weaker board reduction peak b can be observed, too. We can find that when gold was added, the lower temperature reduction peak shifted to the low value of 134 °C, which may be due to the fact that the presence of gold helped to weaken the surface oxygen on ceria-zirconia and thereby improved the reducibility of the catalyst [22]. Flytzani-Stephanopoulos and coworkers [13] suggested that this can facilitate the oxygen transfer across the solid–gas interface during the reaction. We believed that the peaks b and c were attributed to a concomitant reduction of the surface/partially bulk reduction of the support and further reduction of the support in the bulk, respectively. Furthermore, we think the reduction of oxidic gold (Au^{3+}) may exist in the board peak b (420–590 °C), although it was masked by the much higher amount of the surface oxygen associated to the ceria-zirconia.

3.2. Catalytic activity for CO oxidation

The activities of the catalysts for CO oxidation as a function of the reaction temperature are shown in Figs. 7–9. It can be observed that the CO conversion increased with the increasing reaction temperature for all the prepared catalysts. Most of the catalysts began to oxidize CO to CO_2 at 30 °C. In order to search the proper experimental condition, the influence of the pH values, Au contents, calcination temperature and time on the CO oxidation catalytic activity was studied.

3.2.1. Effect of the pH value

Fig. 7 presents the catalytic activity for CO oxidation of the catalysts Au/$Ce_{0.8}Zr_{0.2}O_2$ prepared at different pH values. It is noted that the pH values of the solution had a great influence on the catalytic activity of the catalysts. With the same Au content and calcination condition (300 °C, 3 h), the temperatures of 100% CO conversion ($T_{100\%}$) for these catalysts were different, obviously. The $T_{100\%}$ for the catalysts with pH 6, 7, 8, 9, 10 were 210, 150, 170, 170, 190 °C, respectively. While the catalyst with the pH 5 could not reach the complete conversion and the maximum CO conversion was only 66.0% under the given reaction condition. The XRD analysis results showed that the pH value adjusted in the process of preparation played an important role in the dispersion of gold on the support. When the pH < 7, the Au dispersion degree was lower than that of the samples with pH ≥ 7, which resulted in the inferior activity for the sample with pH 5 and 6. Several groups have reported that the presence of the chloride ions was detrimental to the catalytic property of the catalyst [23–26]. Haruta et al. [24] have reported that when the pH value achieved to above 6, the main Au species was transformed from $AuCl^{4-}$ to $Au(OH)_nCl_{4-n}^-$ ($n = 1$–3). In our present study, the catalytic activity for the catalysts increased from pH 5 to 7, but it decreased when the pH > 7 and the catalyst with pH 7 exhibited a better catalytic activity. According to the above analyses, we think that much chloride ions might

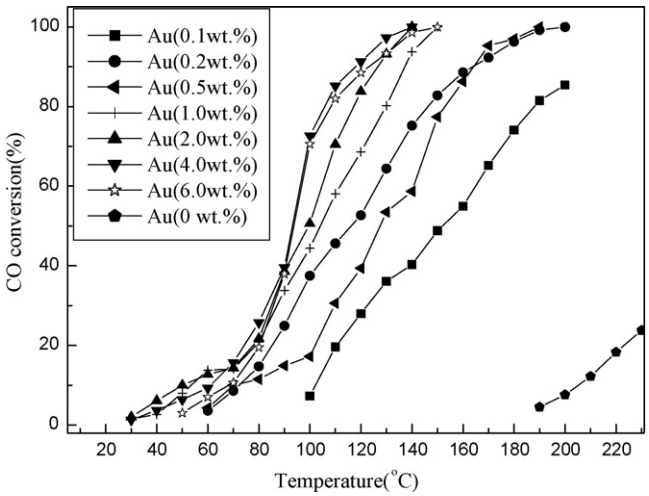

Fig. 8. Catalytic activity of the catalysts Au/$Ce_{0.8}Zr_{0.2}O_2$ with different Au contents.

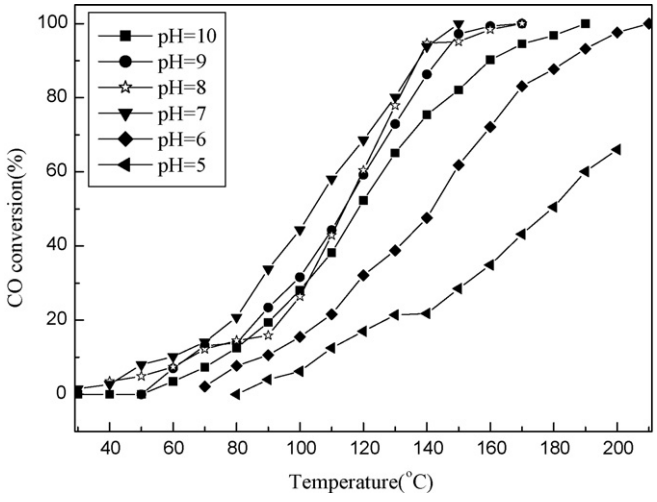

Fig. 7. Catalytic activity for CO oxidation of the catalysts Au/$Ce_{0.8}Zr_{0.2}O_2$ with different pH values.

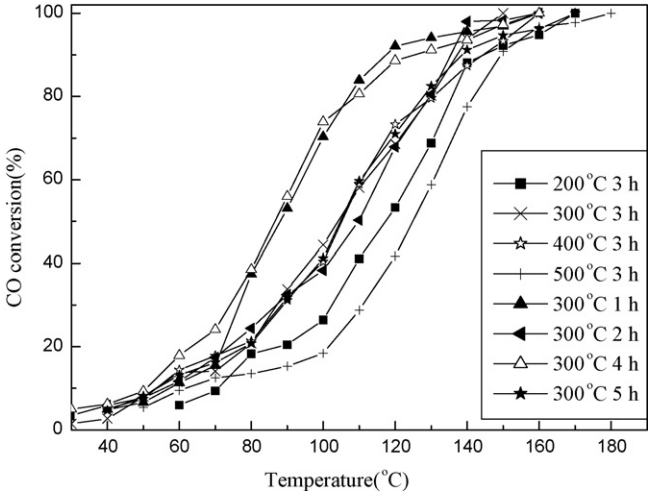

Fig. 9. Catalytic activity of the catalysts Au/$Ce_{0.8}Zr_{0.2}O_2$ with different calcination temperature and calcination time.

associate with the gold complex ions adsorbed on the support at pH 5 and 6, while chloride ions decrease and OH^- increase with increasing pH value. The similar result was reported by Zhu et al. [23]. Therefore, we suggested that pH 7 was a suitable condition to prepare other samples.

3.2.2. Effect of the Au content

The catalytic activity of the catalysts Au/$Ce_{0.8}Zr_{0.2}O_2$ with different Au contents is shown in Fig. 8. It depicted that the activity of the support $Ce_{0.8}Zr_{0.2}O_2$ was quite low, but the Au-loading catalysts showed higher catalytic activities. This indicated that there was a strong interaction between gold and the support, which was responsible for the high CO catalytic activity [13]. In the present case, the addition of gold played an important role in the catalytic performance of the catalysts. The $T_{100\%}$ of the samples with 0.2, 0.5, 1, 2, 4 and 6 wt.% Au loadings were 200, 190, 150, 140, 140 and 150 °C, respectively, and the 0.1 wt.% Au/$Ce_{0.8}Zr_{0.2}O_2$ cannot reach the complete conversion under the experimental condition. The phenomena can be explained by TPR analysis which showed that the addition of gold can weaken the surface oxygen on ceria-zirconia and improve the reducibility of the catalyst [22]. It is noted that the $T_{100\%}$ decreased with the increase of the gold loadings from 0.1 to 2 wt.%, however, it increased when the Au loading increased from 4 to 6 wt.%. This indicated that a well-dispersed state of gold particles on the surface of support was responsible for the superior catalytic property and the agglomeration of gold particles may have negative contribution in the present study, which was in good agreement with the result of XRD and XPS analyses. For the purpose of comparison, the Au(1 wt.%)/$Ce_{0.8}Zr_{0.2}O_2$ was selected to continue the following study.

3.2.3. Effect of the calcination temperature and time

The influence of calcination temperature and calcination time of the catalysts Au(1 wt.%)/$Ce_{0.8}Zr_{0.2}O_2$ (pH 7) on the catalytic activity for low-temperature CO oxidation was investigated and the results are showed in Fig. 9. The different calcination process can lead to different catalytic effect for the catalysts. It is noted that higher calcination temperature and longer calcination time had negative effect on the catalytic activity. It can be found that the catalyst calcined at 300 °C for 3 h showed higher catalytic performance ($T_{100\%}$ = 150 °C). Zhu et al. [23] have reported that higher calcination temperature can accelerates the agglomeration of the gold particles and decrease the activity of catalyst. It can be seen that the $T_{100\%}$ of the sample calcined at 400 and 500 °C for 3 h were 160 and 180 °C, respectively, which were higher than that of the sample calcined at 300 °C. But when the calcination temperature was 200 °C, the $T_{100\%}$ was 170 °C, which showed a decrease in the catalytic activity. We think that at lower temperature, small particles can be obtained but the interaction between gold and the support was weak and influenced the catalytic performance. The catalysts with the treatment at different calcination time showed the similar catalytic performance, the $T_{100\%}$ of the samples calcined 300 °C for 1, 2, 4 h were all 160 °C, but when the calcination time increased to 5 h, the $T_{100\%}$ increased to 170 °C. This may be due to the agglomeration of gold when it was calcined for long time.

From Figs. 7–9, it can be seen that the Au(2 wt.%)/$Ce_{0.8}Zr_{0.2}O_2$ catalyst with pH 7 and calcined at 300 °C for 3 h exhibited the best catalytic performance ($T_{100\%}$ = 140 °C) in the present case. The results indicated that the pH values, Au contents, calcination temperature and time had evident influence on the catalytic performance of the Au-loading catalysts for low-temperature CO oxidation under the experimental conditions.

4. Conclusions

$Ce_{0.8}Zr_{0.2}O_2$ nano-particles and Au/$Ce_{0.8}Zr_{0.2}O_2$ catalysts were successfully prepared by hydrothermal route combined with deposition-precipitation method. XRD and FT-Raman analyses indicated the presence of only the cubic fluorite structure type for the support of the catalysts. The HRTEM measurements showed that the morphology of the samples was spherical. XPS analysis revealed both Ce^{4+} and Ce^{3+} existed on the surface of the catalyst and the Au species presented were Au^0 and Au^{3+}. The study of the catalytic activity for CO oxidation indicated that the catalytic property of the catalysts strongly depended on the pH values adjusted in the process of preparation, gold loadings, calcination temperature and time. It can be observed that the addition of gold can improve the reducibility of the catalyst obviously, which may be due to the weaker bonding of the surface oxygen with ceria-zirconia revealed by TPR analysis [23]. From the XRD and XPS analyses, we think highly dispersed gold particles were responsible for better catalytic activity and the agglomeration of gold particles may have negative contribution. The suitable condition to prepare the catalysts was pH 7 and the optimum thermal pretreatment were 300 °C and 3 h.

References

[1] A. Trovarelli, C. De Leitenburg, M. Boaro, R. Dolcetti, Catal. Today 50 (1999) 353.
[2] K. Min, M.-W. Song, C.H. Lee, Appl. Catal. A 251 (2003) 143.
[3] H.S. Gandhi, G.W. Graham, R.W. McCabe, J. Catal. 216 (2003) 433.
[4] J. Kašpar, P. Fornasiero, N. Hickey, Catal. Today 77 (2003) 419.
[5] S.-P. Wang, X.-C. Zheng, X.-Y. Wang, S.-R. Wang, S.-M. Zhang, L.-H. Yu, W.-P. Huang, S.-H. Wu, Catal. Lett. 105 (2005) 163.
[6] R. Si, Y.-W. Zhang, C.-X. Xiao, S.-J. Li, B.-X. Lin, Y. Kou, C.-H. Yan, Phys. Chem. Chem. Phys. 6 (2004) 1056.
[7] N. Kakuta, S. Ikawa, T. Eguchi, K. Murakami, H. Ohkita, T. Mizushima, J. Alloys Compd. 408–412 (2006) 1078.
[8] H.-L. Chen, H.-Y. Zhu, Y. Wu, F. Gao, L. Dong, J.-J. Zhu, J. Mol. Catal. A 255 (2006) 254.
[9] A. Martorana, G. Deganello, A. Longo, A. Prestianni, L. Liotta, A. Macaluso, G. Pantaleo, A. Balerna, S. Mobilio, J. Solid State Chem. 177 (2004) 1268.
[10] L.F. Chen, G. González, J.A. Wang, L.E. Noreña, A. Toledo, S. Castillo, M. Morán-Pineda, Appl. Surf. Sci. 243 (2005) 319.
[11] J.A. Wang, T. López, X. Bokhimi, O. Novaro, J. Mol. Catal. A 239 (2005) 249.
[12] P.-X. Huang, F. Wu, B.-L. Zhu, X.-P. Gao, H.-Y. Zhu, T.-Y. Yan, W.-P. Huang, S.-H. Wu, D.-Y. Song, J. Phys. Chem. B 109 (2005) 19169.
[13] Q. Fu, S. Kudriavtseva, H. Saltsburg, M. Flytzani-Stephanopoulos, Chem. Eng. J. 93 (2003) 41.
[14] J.E. Spanier, R.D. Robinson, F. Zheng, S.W. Chan, I.P. Herman, Phys. Rev. B 64 (2001) 245407.

[15] A.E. Nelson, K.H. Schulz, Appl. Surf. Sci. 210 (2003) 206.
[16] B.M. Reddy, A. Khan, Catal. Surv. Asia 9 (3) (2005) 155.
[17] M. Alifanti, B. Baps, N. Blangenois, J. Nand, P. Grange, B. Delmon, Chem. Mater. 15 (2003) 395.
[18] M.P. Casaletto, A. Longo, A. Martorana, A. Prestianni, A.M. Venezia, Surf. Interface Anal. 38 (2006) 215.
[19] G.C. Bond, D.T. Thompson, Gold Bull. 33 (2000) 41.
[20] H.C. Yao, Y.F.Y. Yao, J. Catal. 86 (1984) 254.
[21] Y.-M. Kang, B.-Z. Wan, Catal. Today 35 (1997) 379.
[22] U.R. Pillai, S. Deevi, Appl. Catal. A 299 (2006) 266.
[23] B.-L. Zhu, Q. Guo, X.-L. Huang, S.-R. Wang, S.-M. Zhang, S.-H. Wu, W.-P. Huang, J. Mol. Catal. A 249 (2006) 211.
[24] M. Haruta, A. Ueda, S. Tsubota, R.M.T. Sanchez, Catal. Today 29 (1996) 443.
[25] H.H. Kung, M.C. Kung, C.K. Costello, J. Catal. 216 (2003) 425.
[26] F. Moreau, G.C. Bond, A.O. Taylor, Chem. Commun. (2004) 1642.